

### Physicochemical Properties and Antimicrobial Potential of Green Synthesized Cerium Oxide (CeO<sub>2</sub>) Nanoparticles from Pomegranate Peel Extract

S. Sebastiammal<sup>a</sup>, S. Sonia<sup>b</sup>, C. S. Biju<sup>c</sup> and A. Lesly Fathima<sup>b</sup>

<sup>a</sup> Research Scholar (Reg.No:17213042132003), Department of Physics, Holy Cross College (Autonomous), Nagercoil-629004, Tamil Nadu, India. (Affiliated to Manonmaniam Sundaranar University, Abishekapatti, Tirunelveli-627012, Tamil Nadu, India).

<sup>b</sup> Department of Physics, Holy Cross College (Autonomous), Nagercoil-629004, Tamil Nadu, India.

<sup>c</sup> Department of Physics, Malankara Catholic College, Mariagiri, Kaliakkavilai-629 153, Tamil Nadu, India.

**Doi:** <https://doi.org/10.47011/14.1.7>

Received on: 10/02/2020;

Accepted on: 24/04/2020

---

**Abstract:** Green synthesis of CeO<sub>2</sub> Nanoparticles (NPs) with small size and high stability paved the approach to recover and protect the environment by decreasing the use of toxic chemicals and eliminating biological risks in biomedical applications. Peel-mediated synthesis of CeO<sub>2</sub> NPs is gaining more importance owing to its easiness and eco-friendliness. In this study, biosynthesis of CeO<sub>2</sub> NPs using the fruit peel extract of *punica granatum* is reported. The synthesized CeO<sub>2</sub> NPs are characterized by Powder X-ray Diffraction (PXR), UV-Diffused Reflection Spectroscopy (UV-DRS), Field Emission Scanning Electron Microscopy (FESEM), Energy Dispersive X-Ray Analysis (EDAX) and antimicrobial activity. The CeO<sub>2</sub> NPs show more lethal activity towards gram +ve bacteria than towards gram -ve bacteria.

**Keywords:** Biosynthesis, Optical properties, Antimicrobial activity.

## Introduction

Pathogenic microorganisms have become a major problem in our today life, since they pose a threat to health and food materials. This paves the way to the research community to investigate solutions to remove or reduce these hazardous species from the environment. Emergence of new bacterial strains which are resistant to current antibiotics has become a serious health issue. From recent literature, it is believed that nanotechnology is one of the most active research areas in providing solutions for such problems. Synthesis of nanoparticles (NPs) with various sizes and shapes has gained much

importance in nanotechnological applications [1-5]. In general, nanoparticles have a higher surface-to-volume ratio with an enlarged contact area with microbes. This feature enhances the biological activity of NPs and finds applications in the medical field.

CeO<sub>2</sub> is a semiconductor material which has a wide bandgap ranging between 3.0 eV and 3.9 eV with large excitation energy [6]. CeO<sub>2</sub> NPs have received much attention in nanotechnology due to their useful applications as catalysts, fuel cells and antioxidants in biological systems [7-10]. CeO<sub>2</sub> can be prepared by several methods,

such as precipitation [11], hydrothermal method [12], microwave method [13], chemical reduction [14], heat evaporation [15] and electrochemical reduction [16, 17]. In the above methods, hazardous chemicals were used as reducing or stabilizing agents. Hence, there is an emerging need to develop an environment-friendly route to synthesize CeO<sub>2</sub> NPs.

In recent years, green synthesis gained much attention due to its ecofriendly and cost-effective nature. In green synthesis, route plant extracts are mainly employed for the preparation of NPs. There are several reports available for the preparation of CeO<sub>2</sub> NPs by green synthesis method. In green synthesis, for the preparation of

CeO<sub>2</sub> NPs, the authors used *Hibiscus sabdariffa* flower [7], *Olea europaea* leaf [18], *Prosopis juliflora* leaf [6], *Moringa olifera* seeds [19], *Gloriosa superba* L. leaf [10], *Momordica charantia* leaf [20], *Acalypha indica* leaf [21] and *Morus nigra* fruit [22]. The authors reported the structural, optical and antibacterial characteristics of CeO<sub>2</sub> NPs. The antibacterial property varies with the various plant extracts. The use of pomegranate peel extract for the preparation is unanswered. This motivated the authors to study the physicochemical and antimicrobial properties of pomegranate (*Punica granatum*) peel extract-mediated CeO<sub>2</sub> NPs.

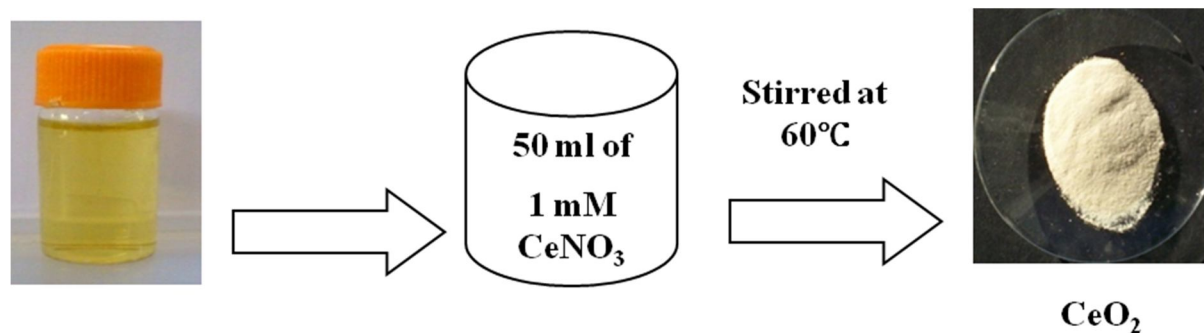


FIG. 1. Synthesis of CeO<sub>2</sub> NPs using 10 ml of *Punica granatum* peel extract.

Pomegranate has a mixture of various bioactive compounds and is being used as a folk medicine for years. Pomegranate seeds, peels and fruits play a role in disease cure through modulation of biological activities [23]. The *Punica granatum* peel is a rich source of flavonoids, tannins and many phenolic compounds. The pomegranate peel has the highest antioxidant activity when compared to the seed and the pulp [24]. Pomegranate peel extract (PPE) efficiently reduces AgNO<sub>3</sub> into Ag<sup>+</sup> ions [25], Fe<sup>3+</sup> ions into Fe<sup>0</sup> [26] and Zinc ions into nanoparticles [23]. Also, PPE is used to prepare silver nanoparticles at room temperature [27]. The reducing ability of the peel extract for the synthesis of nanoparticles is due to its higher polyphenolic content [28]. Several researchers employed PPE for the preparation of NPs, such as NiFe NPs [28], ZnO NPs [23], Ag NPs [25, 27], Au NPs [29], Cu NPs [30] and Fe<sub>3</sub>O<sub>4</sub> NPs [31]. Hence, the present work is aimed to prepare CeO<sub>2</sub> NPs by pomegranate peel extract and to study their physicochemical and antimicrobial properties.

## Experimental Details

### Preparation of Extracts

10 g of fresh peels of *Punica granatum* were incised into fine pieces and transferred into a beaker containing 50 ml of double distilled water. The mixture was allowed to boil at 80 °C for 3 min. and thus obtained extracts were filtered using Whatman No. 1 filter paper.

### Synthesis of CeO<sub>2</sub> Nanoparticles

10 ml of peel extracts were added to 1mM aqueous solution of Ce(NO<sub>3</sub>)<sub>2</sub> dissolved in 50 ml of double distilled water. The reaction mixture was stirred vigorously for 30 minutes. The solution was then heated on a hot plate at 80 °C till the supernatant got evaporated. The obtained product was pounded into fine powder and calcinated at 600 °C for 2 hours. The synthesized CeO<sub>2</sub> NPs sample is pale yellow in color.

### Characterization Technique

The crystal structures of the obtained products were characterized by studying the X-ray diffraction pattern (PANalytical X'pert Pro with CuK<sub>α</sub> (λ=1.5406 Å)). FTIR spectroscopic analysis was performed using the KBr pellet

method (model SHIMADZU FTIR, Kyoto, Japan) in the wavenumber range 400–4,000 cm<sup>-1</sup>. The morphology and elemental composition of the samples were analyzed using a field emission scanning electron microscope (FEI QUANTA-250). Optical studies were recorded using UV-Diffused reflection spectroscopy (JASCO V-650 Spectrophotometer).

### Antibacterial Test

Antibacterial activity of the synthesized CeO<sub>2</sub> Nanoparticles was determined using the well diffusion method. It was performed by sterilizing Mueller Hinton agar (MHA) media. After solidification, wells were cut on the MHA plates using a cork borer and the test bacterial pathogens were swabbed onto the surface of MHA plates. The samples were placed on the well and the plates were incubated at 37° C for 24 hrs. The zone of inhibition was measured in millimeters. Each antibacterial assay was

performed in triplicate and mean values were reported.

## Structural Characterization of CeO<sub>2</sub>NPs

### Powder X-Ray Diffraction Studies

The phase purity, crystal structure, average crystalline size and dislocation density were determined through XRD analysis. Fig.2 shows the XRD pattern of CeO<sub>2</sub> NPs prepared using PPE and shows diffraction peaks at 2θ = 28.589°, 33.130°, 47.556°, 56.431°, 59.183°, 69.529° and 76.832° corresponding to (111), (200), (220), (311), (222), (400) and (331) planes of cubic structured CeO<sub>2</sub> (JCPDS card No. 65-5923). The obtained result is in good agreement with the earlier report for the CeO<sub>2</sub> NPs prepared by green synthesis [32].

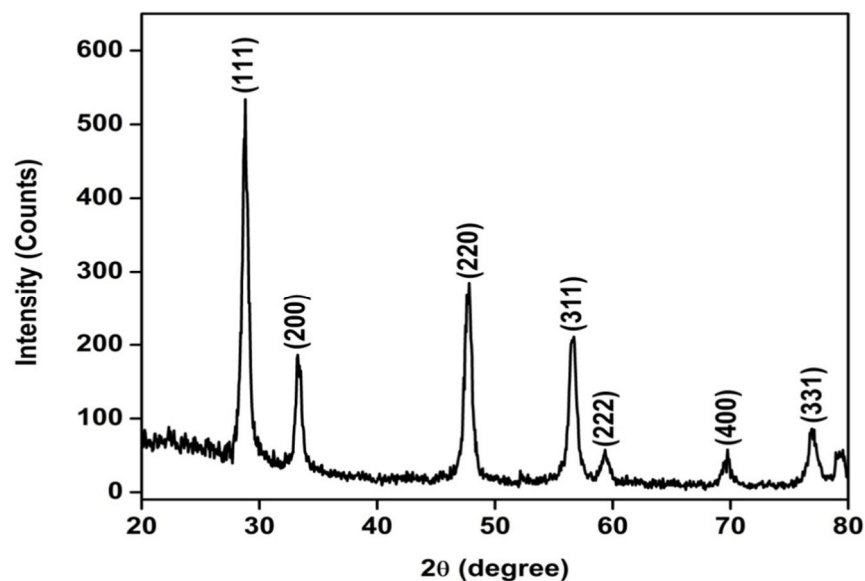


FIG. 2. PXRD spectrum of CeO<sub>2</sub> NPs using *Punica granatum* peel extract.

The average crystallite size was calculated using Scherrer's formula [33]:

$$D = \frac{0.9\lambda}{\beta \cos\theta} \text{ (nm)} \quad (1)$$

where D- crystallite size, k- shape factor (0.9) and λ- wave length of CuK<sub>α</sub> radiation. β is the full width at half maximum of the dominant peak and θ is the Bragg angle. The lattice parameter (a) and cell volume were calculated using the unit cell software. The dislocation density was calculated by using the relation [34]:

$$\delta = \frac{1}{D^2} \text{ (lines m}^{-2}\text{)}. \quad (2)$$

The average crystallite size and dislocation density were found to be 21 nm and 2.26 x 10<sup>15</sup> lines/m<sup>2</sup>, respectively. The lattice parameter value is found to be about a = 5.403 Å. The obtained unit cell value is in good agreement with the JCPDS card No. 65-5923. From the XRD pattern, it is proved that the biosynthesis using PPE is able to produce CeO<sub>2</sub> NPs.

### FTIR Analysis

Fig. 3 displays the FT-IR spectrum of CeO<sub>2</sub> nanoparticles. The strong peaks around 2857.85 cm<sup>-1</sup> and 2925.03 cm<sup>-1</sup> were attributed to O–H

stretching and C–H stretching, respectively. The Ce - O stretching band observed at  $452.73\text{ cm}^{-1}$  confirms the formation of  $\text{CeO}_2$ . Similarly, Ce–O stretching bands at  $451\text{ cm}^{-1}$ ,  $459\text{ cm}^{-1}$  and  $450\text{ cm}^{-1}$  were reported by Arumugam *et al.*, Q.Maqbool *et al.* and Goharshadi *et al.*, respectively [10, 18]. The peak at  $3753.65\text{ cm}^{-1}$

corresponds to the physically adsorbed water molecules. Furthermore, the absorption band at  $1638.92\text{ cm}^{-1}$  was related to the presence of N-H bending of primary amines. N–O symmetric stretch at  $1,379.78\text{ cm}^{-1}$  was indicating that Ce is actively oxidized to  $\text{CeO}_2$  by the nitro-compounds.

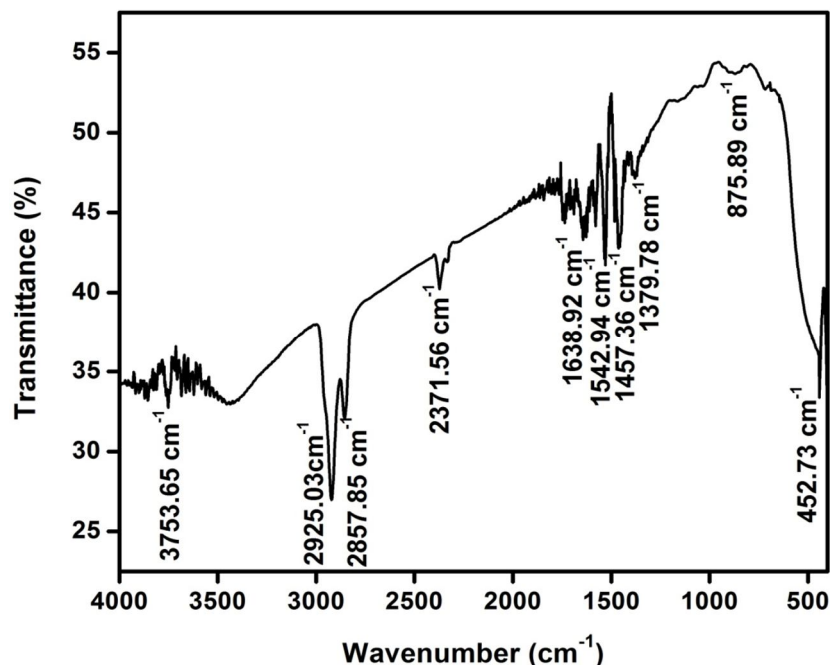


FIG. 3. FTIR spectrum of  $\text{CeO}_2$  NPs using *Punica granatum* peel extract.

### Field Emission Scanning Electron Microscopy Analysis

The morphology and pore size of the synthesized  $\text{CeO}_2$  NPs were observed using FESEM. Fig.4 (a-d) shows the FESEM micrograph of  $\text{CeO}_2$  NPs with different magnifications (10,000X, 20,000X, 40,000X and 80,000X). FESEM micrograph of  $\text{CeO}_2$  shows irregular morphology with porous structure with pore size being about  $\sim 200\text{ nm}$ . Moreover, a slight agglomeration was observed that may be due to the Van der Waals force of attraction between the individual  $\text{CeO}_2$  NPs. Zhen Wang *et al.* reported that the porous structure is important for tissue reconstruction and regeneration processes [35], as well as for drug delivery [36].

### Energy Dispersive X-ray Analysis

The elemental composition of  $\text{CeO}_2$  NPs was obtained by EDAX equipped with FESEM. The EDAX analysis of  $\text{CeO}_2$  NPs is given in Fig. 5, which shows strong signals for Ce and O. The elemental compositional values of Ce and O were found to be about 87.76 and 12.24, respectively, which shows oxygen vacancies

created in the system. No other impurities are found in the EDAX spectrum, which shows the purity of the sample.

### Optical Characterization

In order to study the optical properties of  $\text{CeO}_2$  NPs, the prepared nanoparticles were subjected to UV-DRS spectroscopy. The absorbance, transmittance and reflectance spectra of the  $\text{CeO}_2$  NPs are given in Fig.6. In the absorption spectrum (Fig. 6a), the  $\text{CeO}_2$  NPs shows maximum absorption at  $361\text{ nm}$  and thereby it gets decreased in the visible region. The  $\text{CeO}_2$  NPs higher absorption at  $200\text{ nm}$ -  $400\text{ nm}$  indicates that the absorption of  $\text{CeO}_2$  nanoparticles is in the UV region. The transmission spectrum (Fig. 6b) shows higher optical transmission in the visible region, which shows that the prepared  $\text{CeO}_2$  NPs are a wide-bandgap semiconductor and can be used as a window material for photovoltaic applications. The reflectance spectrum of  $\text{CeO}_2$  nanoparticles is given in Fig. 6c. It is apparent from the spectrum that the absorption threshold edge of  $\text{CeO}_2$  nanoparticles is observed at  $360\text{ nm}$ .

The optical band gap energy ( $E_g$ ) of the CeO<sub>2</sub> nanoparticles was estimated using the equation [37]:

$$\alpha h\nu = A (h\nu - E_g)^n \quad (3)$$

where,  $\alpha$  is the absorption coefficient,  $h\nu$  is the discrete photon energy,  $A$  is a constant and  $E_g$  is the band gap of the material. The value of  $n$  is  $\frac{1}{2}$  and  $2$  for direct allowed and indirect allowed transitions, respectively. The band gaps of the samples can be obtained by plotting  $(\alpha h\nu)^2$  versus  $h\nu$  in the high absorption range followed

by extrapolation of the linear portion of the absorption edge to find the intercept on the X-axis, as shown in Fig.6 (d). The bandgap value is found to be 3.72 eV for CeO<sub>2</sub> NPs. The obtained band gap value agrees well with the earlier report of CeO<sub>2</sub> NPs. The obtained bandgap value is found to be lower than those of the CeO<sub>2</sub> nanoparticles prepared using *Momordica charantia* leaf extract [20] and *Gloriosa superb* leaf extract [10]. Also, the bandgap is red-shifted compared with bulk CeO<sub>2</sub> ( $E_g = 3.19$  eV).

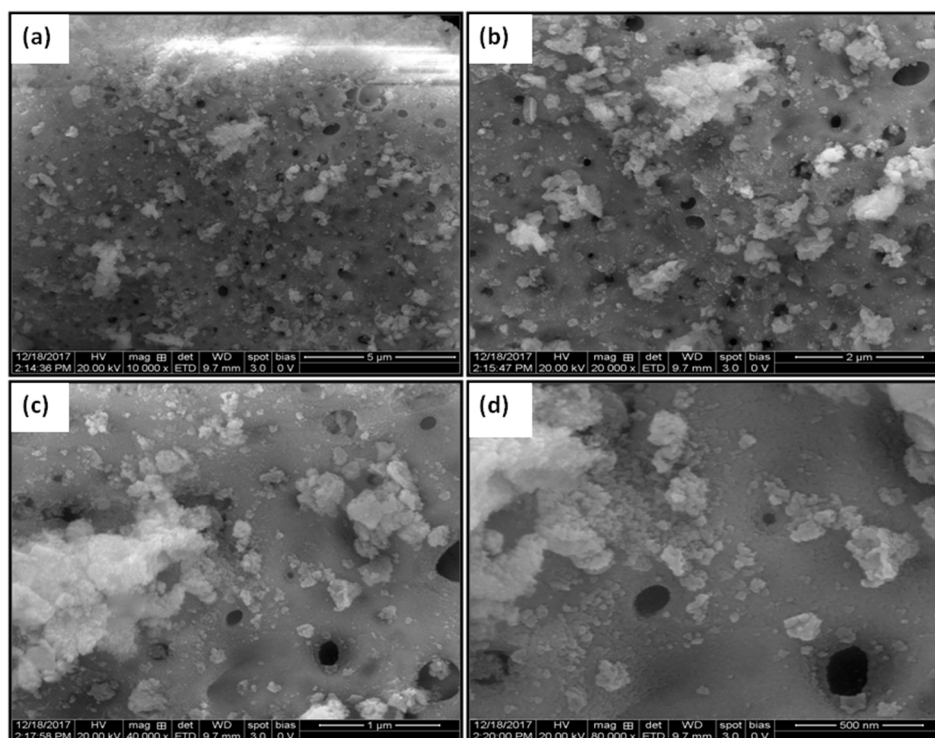


FIG. 4. FESEM image of CeO<sub>2</sub> nanoparticles at a) 10,000X, b) 20,000X, c) 40,000X and d) 80,000X magnifications.

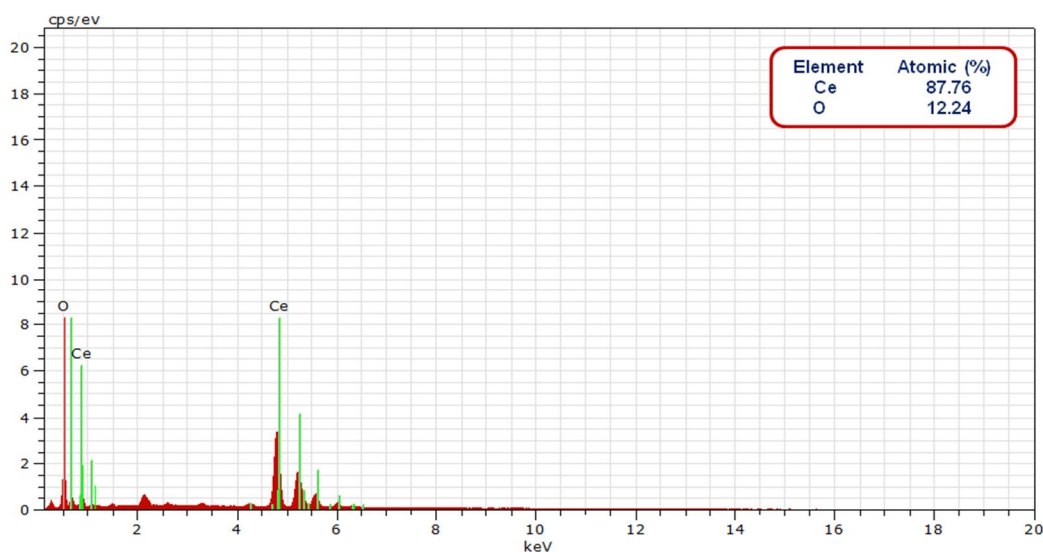


FIG. 5. EDAX spectra for CeO<sub>2</sub> nanoparticles with *Punica granatum* peel extract.



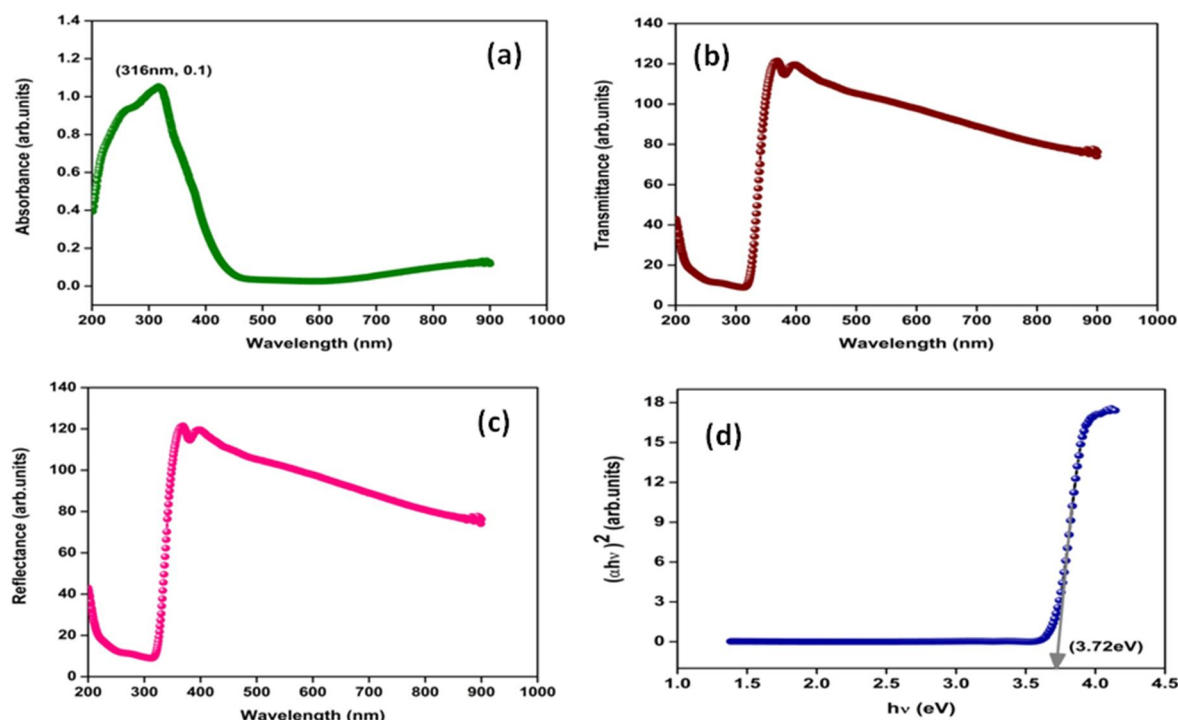


FIG.6. UV-DRS spectra of CeO<sub>2</sub> NPs a) Absorbance, b) Transmittance, c) Reflectance and d) Tauc plot.

### Antimicrobial Activity of CeO<sub>2</sub> NPs

The antimicrobial activity of CeO<sub>2</sub> NPs using *Punica granatum* peel extract was investigated towards various pathogens, such as *S. aureus*, *S. mutans*, *K. pneumonia*, *P. vulgaris*, *A. flavus* and *A. nigar* by the agar diffusion method. The sizes of the zone of inhibition are presented in Table 1. In the present study, the maximum zone of inhibition was observed in the CeO<sub>2</sub> NPs with n-butanol against *S. aureus* (10mm), *S. mutans* (11mm), *K. pneumonia* (9mm), *P. vulgaris* (10mm), *A. flavus* (8mm) and *A. nigar* (8mm), as shown in Fig. 7. Interaction between the nanoparticles and the cell walls of bacteria confirms the fact that the growth of *gram-*

*positive* bacterial strains was more affected by CeO<sub>2</sub> NPs than that of *gram-negative* bacterial strains. This shows that the CeO<sub>2</sub> NPs possess a higher effective lethal activity towards gram +ve bacteria than gram –ve bacteria as reported by Q. Maqbool. The antibacterial activity of CeO<sub>2</sub> NPs depends on the size, morphology and specific surface area. Based on the concept, smaller particles have larger surface areas for interaction and will have a stronger bactericidal effect than larger particles. The synthesized CeO<sub>2</sub> NPs have greater antibacterial activity [38, 39]. Also, electromagnetic interaction and ROS generation might render CeO<sub>2</sub> NPs as potential antibacterial agents.

TABLE 1. Antibacterial activity of CeO<sub>2</sub> NPs via *Punica granatum* peel extract calcined at 600 °C.

Sample name/ Solvents	Strains					
	<i>S. aureus</i>	<i>S. mutans</i>	<i>K. pneumoniae</i>	<i>P. vulgaris</i>	<i>A. flavus</i>	<i>A. niger</i>
Ce /n-but	10	11	9	10	8	8
Control	22	21	12	14	22	26

### Conclusion

A simple, green and inexpensive technique has been adopted to prepare CeO<sub>2</sub> NPs using *Punica granatum* peel extract as a better alternative to chemical synthesis without using any hazardous chemicals. The PXRD result confirms the formation of face-centered cubic phase structure of CeO<sub>2</sub> NPs. The crystallite size of nanoparticles is estimated at about 21.5483

nm for CeO<sub>2</sub> NPs. FESEM images showed that the synthesized CeO<sub>2</sub> NPs are of nanoporus morphology. UV-DRS analysis shows blue shift, which is due to quantum confinement effect. The maximum zone of inhibition was observed in the CeO<sub>2</sub> NPs with n-butanol against *S. aureus*, *S. mutans*, *K. pneumonia*, *P. vulgaris*, *A. flavus* and *A. nigar* as tested by the agar diffusion method. The CeO<sub>2</sub> NPs prepared from PPE possess good antimicrobial activity.

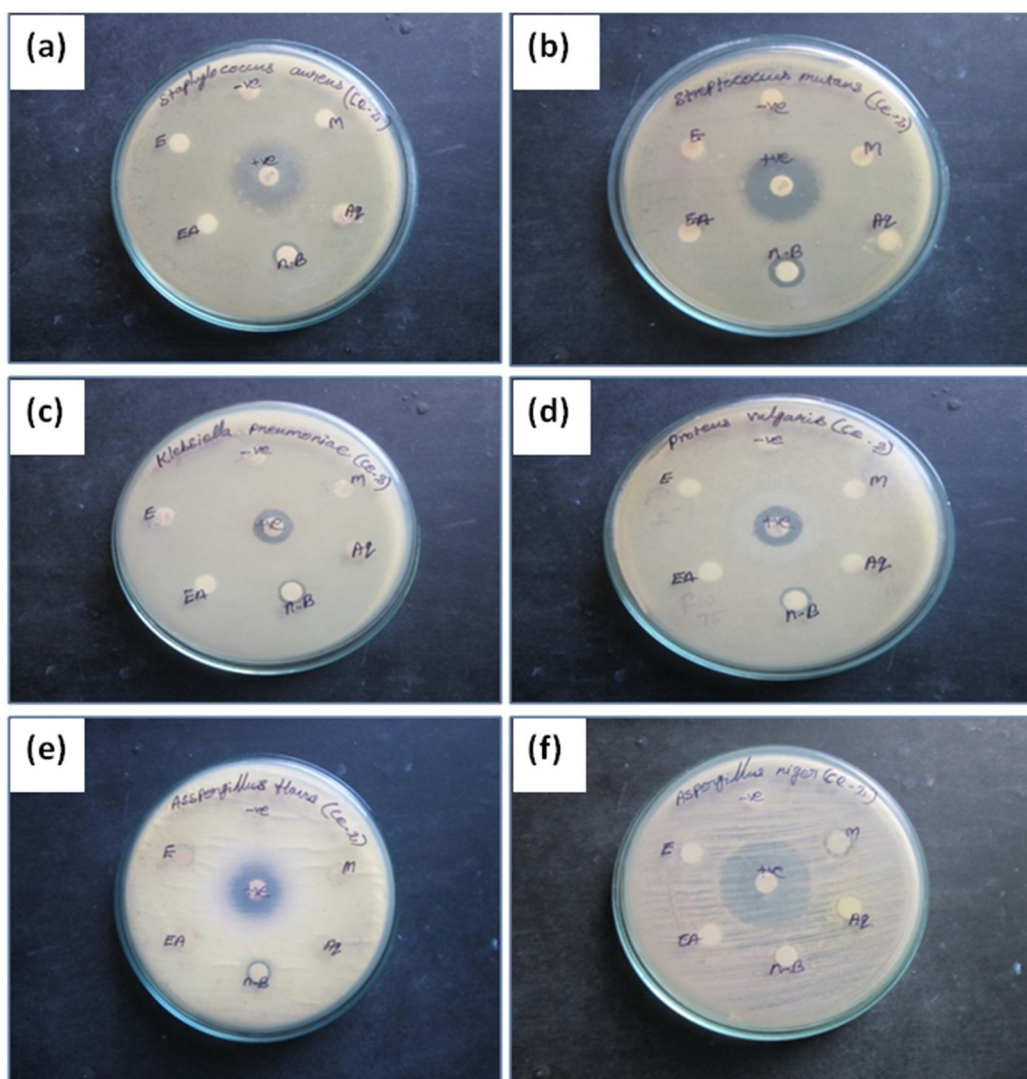


FIG. 7. Zone of inhibition of CeO<sub>2</sub> NPs synthesised via *Punica granatum* peel extract against a) *S. aureus*, b) *S. mutans*, c) *K. pneumoniae*, d) *P. vulgaris*, e) *A. flavus* and f) *A. niger*.

## References

- [1] Henry, J., Mohanraj, K. and Sivakumar, G., *Journal of Inorganic and Organometallic Polymers and Materials*, 26 (2016) 312.
- [2] Rajiv, P., Rajeshwari, S. and Venckatesh, R., *Spectrochimica Acta - Part A: Molecular and Biomolecular Spectroscopy*, 112 (2013) 384.
- [3] Nagajyothi, P.C., Sreekanth, T.V.M., Tetey, C.O., Jun, Y.I. and Mook, S.H., *Bioorganic & Medicinal Chemistry Letters*, 24 (2014) 4298.
- [4] Salam, H.A., Sivaraj, R. and Venckatesh, R., *Materials Letters*, 131 (2014) 16.
- [5] Zak, A.K., Majid, W.H.A., Mahmoudian, M.R., Darroudi, M. and Yousefi, R., *Advanced Powder Technology*, 24 (2013) 618.
- [6] Arunachalam, T., Karpagasundaram, M. and Rajarathinam, N., *Materials Science-Poland*, 35 (2017) 791.
- [7] Thovhogi, N., Diallo, A., Gurib-Fakim, A. and Maaza, M., *Journal of Alloys and Compounds*, 647 (2015) 392.
- [8] Yu, L. and Xi, J., *International Journal of Hydrogen Energy*, 37 (2012) 15938.
- [9] Nurhasanah, I., Safitri, W., Arifin, Z., Subagio, A. and Windarti, T., *IOP Conf. Ser.: Mater. Sci. Eng.*, 432 (2018) 012031.
- [10] Arumugam, A., Karthikeyan, C., Hameed, A.S.H., Gopinath, K., Gowri, S. and Karthika, V., *Materials Science and Engineering C*, 49 (2015) 408.

- [11] Farahmandjou, M., Zarinkamar, M. and Firoozabadi, T.P., *Revista Mexicana de Fisica*, 62 (2016) 496.
- [12] Panahi-Kalamuei, M., Alizadeh, S., Mousavi-Kamazani, M. and Salavati-Niasari, M., *Journal of Industrial and Engineering Chemistry*, 21 (2015) 1301.
- [13] Kumar, E., Selvarajan, P. and Balasubramanian, K., *Recent Research in Science and Technology*, 2 (2010) 37.
- [14] Yu, D.G., *Colloids and Surfaces - B: Biointerfaces*, 59 (2007) 171.
- [15] Smetana, A.B., Klabunde, K.J. and Sorensen, C.M., *Journal of Colloid and Interface Science*, 284 (2005) 521.
- [16] Liu, Y.C. and Lin, L.H., *Electrochemistry Communications*, 6 (2004) 1163.
- [17] Mallick, K., Witcomb, M.J. and Scurrall, M.S., *Materials Chemistry and Physics*, 90 (2005) 221.
- [18] Qaisar, M., Nazar, M., Naz, S., Hussain, T., Jabeen, N., Kausar, R., Anwaar, S., Abbas, F. and Jan, T., *International Journal of Nanomedicine*, 11 (2006) 5015.
- [19] Mahmud, S.A., *International Journal of Chemical and Biochemical Sciences*, 10 (2016) 37.
- [20] Anand, B., Muthuvel, A., Mohana, V., Anandhi, S. and Pavithra, M., *International Journal for Research in Applied Science & Engineering Technology (IJRASET)*, 6 (2018) 1073.
- [21] Kannan, S.K. and Sundrarajan, M., *International Journal of Nanoscience*, 13 (2014) 1450018.
- [22] Rajan, A.R., Rajan, A., John, A. and Philip, D., *AIP Conference Proceedings*, 2105 (2019) 020008.
- [23] Husain, W.M., Araak, J.K. and Ibrahim, O.M.S., *The Iraqi Journal of Veterinary Medicine*, 43 (2019) 6.
- [24] Li, Y., Guo, C., Yang, J., Wei, J., Xu, J. and Cheng, S., *Food Chemistry*, 96 (2006) 254.
- [25] Fernandes, R.A., Berretta, A.A., Elina Cassia Torres, E.C., Buszinski, A.F.M., Fernandes, G.L., Mendes-Gouvêa, C.C., Souza-Neto, F.N.D., Gorup, L.F., Camargo, R.R.D. and Barbosa, D.B., *Antibiotics*, 7 (2018) 1.
- [26] Al-Timmimi, S.S., *International Journal of Science and Nature*, 8 (2017) 213.
- [27] Joshi, S.J., Geetha S.J, Al-Mamari, S. and Al-Azkawi, A., *Jundishapur J. Nat. Pharm. Prod.*, 13 (2018) e67846.
- [28] Ravikumar, K.V.G., Sudakaran, S.V., Ravichandran, K., Pulimi, M., Natarajan, C. and Mukherjee, A., *Journal of Cleaner Production*, 210 (2019) 767.
- [29] Ahmad, N., Sharma, S. and Rai, R., *Adv. Mater. Lett.*, 3 (2012) 376.
- [30] Kaur, P., Thakur, R. and Chaudhury, A., *Green Chemistry Letters and Reviews*, 9 (2016) 33.
- [31] Venkateswarlu, S., Kumar, B.N., Prathima, B., Rao, Y.S. and Jyothi, N.V.V., *Arabian Journal of Chemistry*, 12 (2019) 588.
- [32] Charbgoon, F., Ahmad, M. and Darroudi, M., *International Journal of Nanomedicine*, 12 (2017) 1401.
- [33] Henry, J., Mohanraj, K. and Sivakumar, G., *Jordan J. Phys.*, 11 (2018) 101.
- [34] Henry, J., Ajaypraveenkumar, A., Sivakumar, G. and Mohanraj, K., *Journal of Central South University*, 24 (2017) 2793.
- [35] Wang, Z., Chang, J., Bai, F., Sun, X., Lin, K., Chen, L., Lu, J. and Dai, K., *Nature Proceedings* (2010) DOI: 10.1038/npre.2010.4148.1
- [36] Michailidis, N., Tsouknidas, A., Lefebvre, L.P., Hipke, T. and Kanetake, N., *Advances in Materials Science and Engineering*, 2014 (2014) 263129.
- [37] Henry, J., Mohanraj, K. and Sivakumar, G., *Journal of Physical Chemistry - C*, 123 (2019) 2094.
- [38] Ramesh, M., Anbuvaran, M. and Viruthagiri, G., *Spectrochimica Acta - Part A: Molecular and Biomolecular Spectroscopy*, 136 (2015) 864.
- [39] Saravanakumar, A., Ganesh, M., Jayaprakash, J. and Jang, H.T., *Journal of Industrial and Engineering Chemistry*, 25 (2015) 277.